Channel models in the near field

Akl Charaf, *Member, IEEE* and Georges R. Guisantes, *Member, IEEE.*

***Abstract*—We present in this work the state of the art of near field communications (NFC) systems channel models. We proceed by proposing a new model and compare the performance with the most frequently used ones.**

***Index Terms*—Near and far field path loss models, inductive channel, NFC communications systems, secure NFC systems.**

I. Introduction

NO one can ignore the great importance of the development of connected objects. These new technologies are boosting economic actors to develop smarter devices enabling a massive connectivity to INTERNET thus creating new business models and services. The INTERNET of Things (IoT)is considered as a new deal for the 5G cellular systems [1]. It is clear that in IoT, the bulk of traffic will come from technologies that communicate in the proximity of objects (such as RFID, NFC and low power/short range technologies). Beyond this fact, the technology of the near field communication systems has some special characteristics: *physical security* provided by the low range coverage area of induction and its non-propagating nature; *low consumption* devices, with currents between $10\,\mu\mathrm{A}$ and $100\,\mu\mathrm{A}$ [2]; *low manufacturing costs*; *simplicity of use*; and the possibility of *embedded solutions* in other devices, such as smartphones. In the far field, the electromagnetic (EM) wave propagates as described by Maxwell's equations. Unfortunately, the description of the near field is a complex issue and the fundamental transmission parameters of the equivalent channel are difficult to establish. In the neighborhood of the radiating element, the EM wave behaviour can be described in terms of reactance [3]. This justifies the use of circuit theory to define the channel model, and evaluate the global performance of a digital transmitter/receiver system by a simple power link budget. In this work, we analyze existing circuit models and point out some of their limitations. A modified circuit model is also presented to overcome the highlighted limitations. In section II, we present the existing channel models. In section III, we propose the modified one and we compare their performances. Conclusions and perspectives are presented in section IV.

II. Channel Path Loss Models

NFC is a very popular short and medium range application of the magneto-inductive (MI) communication. MI communication is particularly well adapted to media where acoustic or electromagnetic waves fail to propagate such as communications in underwater and underground [4] [5]. Magneto-inductive communications channel models use an equivalent RLC circuit representation. Over the first fraction of a wavelength distance, the EM field has a very complex and rich structure, both in spatial and temporal domains. The description of the "stored energy", defined as the difference between the total energy and the radiated far field can be interpreted in several ways. Recently, a detailed study of near field structure has been done [3]. The presence of a pseudo-reactive component of the EM field can be approximated by lumped parameters. We present in [6] a detailed analysis of different models based on the descriptions of the EM wave in the near zone.

In the following, we present a more accurate model based on the idea that the near field can be modeled as a linear circuit with lumped parameters and a simple magnetic coupling between the transmitter and the receiver.

Figure 1(a) gives a geometric description of a near field transmission system. It is composed of two axially aligned circular coils of radius a_t (resp a_r), with N_t (resp N_r) turns of wire with linear resistance $R_0\ \Omega.m^{-1}$, separated by a distance d. The coil thickness is assumed to be very small. The transmitting coil is fed by a signal of angular frequency $\omega\ \mathrm{rad\,s^{-1}}$. The transmitting and receiving coil self-inductances are L_t and L_r respectively, while μ is the medium permeability. The magnetic coupling (M) between the coils is:

$$M = \frac{\mu\pi N_t a_t^2 N_r a_r^2}{2\sqrt{(a_t^2+d^2)^3}}. \tag{1}$$

The coupling coefficient k, defined as the efficiency of energy transfer from the transmitting to the receiving coil, is:

$$k = \frac{M}{\sqrt{L_t L_r}}. \tag{2}$$

We define de path loss of this channel as :

$$PL = \frac{Pr}{Pt},$$

or in dB:

$$PL(dB) = -10\log_{10}\frac{Pr}{Pt}.$$

In the following, we analyze different path loss models, corresponding to this geometry.

A. Path loss Model-1 ([7])

The MI channel can be modeled using a RLC lumped parameters circuit as shown in Fig. 2. Z_t and Z_r are (respectively transmitter and receiver) intrinsic complex impedances[1], while Z_t' and Z_r' represent the reflected impedances on each side. M is the mutual inductance between the coils (Eq. 1):

$$Z_t = R_t + j\omega L_t, \quad Z_t' = \frac{\omega^2 M^2}{R_r + j\omega L_r + Z_L}, \tag{3}$$

$$Z_r = R_r + j\omega L_r, \quad Z_r' = \frac{\omega^2 M^2}{R_t + j\omega L_t}. \tag{4}$$

[1] $j = \sqrt{-1}$.

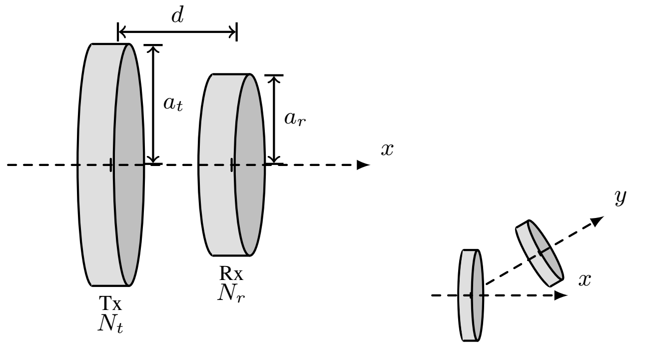

(a) Axially coupled (b) Non-axially coupled

Fig. 1. Geometry of the two magnetically coupled coils

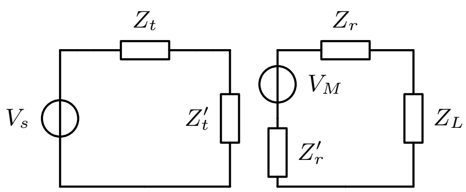

Fig. 2. Equivalent circuit model

The induced voltage in the receiver is:

$$V_M = \frac{-j\omega M V_s}{Z_t}. \tag{5}$$

Using the equivalent circuit model of Fig. 2, the transmitted and received power, P_t and P_r, are given by[2]:

$$P_t = Re(\frac{{V_s}^2}{Z_t + Z'_t}), \quad P_r = Re(\frac{{V_M}^2}{Z_r + Z'_r + Z_L}). \tag{6}$$

In [7], self-inductances are approximated by:

$$L_t = \frac{1}{2}\mu\pi N_t^2 a_t, \quad L_r = \frac{1}{2}\mu\pi N_r^2 a_r. \tag{7}$$

Combining equations (3) to (7) leads to the following path loss (PL) expression (Model-1 in [7]) in load matching condition and assuming $a_r \ll r$ and $\omega\mu N_t \gg R_0$:

$$PL = \frac{P_r}{P_t} \simeq \frac{\omega\,\mu\,N_r\,{a_t}^3\,{a_r}^3}{16\,R_0\,d^6}. \tag{8}$$

It can be noticed that PL is independent of Nt.

B. Path Loss Model-2 ([8])

A two-port network representation of an inductive system can be described by its impedance matrix:

$$\begin{bmatrix} V_1 \\ V_2 \end{bmatrix} = \begin{bmatrix} Z_{11} & Z_{12} \\ Z_{21} & Z_{22} \end{bmatrix} \begin{bmatrix} I_1 \\ I_2 \end{bmatrix}.$$

The MI transmitted power depends on d since the mutual coupling decreases with distance[3]:

$$P_t(d) = Re(V_1 I_1^*) = Re(Z_{11} - \frac{Z_{12}^2}{Z_L + Z_{22}})|I_1|^2 \tag{9}$$

[2] $Re(.)$ represents the real part of a complex.
[3] I^* is the conjugate complex of I.

and the received power is:

$$P_r = Re(Z_L)|I_2|^2 = Re(Z_L)\frac{|Z_{12}|^2}{|Z_L + Z_{22}|^2}|I_1|^2 \tag{10}$$

where

$$\begin{gathered} Z_{11} = R_t + j\omega L_t, \quad Z_{22} = R_r + j\omega L_r, \\ Z_{12} = Z_{21} = j\omega M. \end{gathered} \tag{11}$$

In [8], the authors assume a very small distance d_0 between coils.

$$P_t(d_0) = Re(Z_{11})|I_1|^2. \tag{12}$$

Combining equations (9) to (12) together with the load matching condition leads to the following path loss expression:

$$\frac{P_r}{P_t(d_0)} = \frac{R_L \omega^2 M^2}{R_t(R_L + R_r)^2 + R_t(X_L + \omega L_r)^2} \tag{13}$$

where

$$R_L = R_r + \frac{\omega^2 M^2 R_t}{{R_t}^2 + \omega^2 L_t^2}, \text{ and } X_L = \frac{\omega^3 M^2 L_t}{R_t^2 + \omega^2 L_t^2} - \omega L_r. \tag{14}$$

C. Path Loss Model-3 ([9])

PL can be given in terms of transmitting and receiving coil quality factors (Q_t, resp Q_r) and the coupling factor k defined in Eq. (2):

$$\frac{P_r}{P_t} = k^2 Q_t Q_r, \quad \text{with } Q_t = \frac{\omega L_t}{R_t}, \quad Q_r = \frac{\omega L_r}{R_r}. \tag{15}$$

For a coil of radius a, with N turns of wire, with linear resistance R_0, the self-inductance and resistance are:

$$L = \mu\frac{\pi a N^2}{2\pi N + 0.9} \approx \frac{1}{2}\mu a N, \quad R = 2\pi a N R_0. \tag{16}$$

Assuming $2\pi N \gg 0.9$ and a very small transmitting coil radius compared to the separating distance ($a_t \ll d$), the coupling factor and the path loss are:

$$k^2 = \frac{\pi^2 {a_t}^3 {a_r}^3}{N_t N_r d^6}, \text{ and } \frac{P_r}{P_t} = k^2 Q_t Q_r = \frac{\omega^2 \mu^2 {a_t}^3 {a_r}^3}{16 N_t N_r {R_0}^2 d^6}. \tag{17}$$

III. Modified Path Loss Model and Results

Analysis of a "Modified-model"

Designing a suitable transmitter and receiver for enhanced MI performance requires a better description of the channel behaviour. Models 1, 2 and 3 use approximations leading to simpler expressions at the expense of generality. In addition, the PL expression in Model-2 (Eq. (13)) evaluates the transmitted power at a distance $d_0 \approx 0$, which makes it unsuitable to establish a MI link budget. We notice that these models make use of different self-inductance approximations, which may mask the effect of some system parameters, leading to erroneous results. In the near field, as d gets larger, the mutual coupling (M) decreases (Eq. (9)). Equation (13) is only suitable for comparison between radiated EM waves since it assumes the transmitted power to be independent of distance. A more accurate path loss expression should take into account the real transmitted power in terms of distance. We now consider Eq.

(9), (10), (11) and (14), and derive a new approximation-free PL expression in load matching conditions (see appendix A for details)

$$PL = \frac{P_r}{P_t(d)} = \frac{R_L \omega^2 M^2}{R_t(R_L + R_r)^2 + R_t(X_L + \omega L_r)^2 + \omega^2 M^2 (R_L + R_r)}. \tag{18}$$

This equation is quite similar to Eq. (13), with the major difference of considering the real transmitted power. This transmitted power depends on the distance which makes appear an additional term $\omega^2 M^2 (R_L + R_r)$ in the denominator of Eq. (18).

Equation (1) applies if we assume that both transmitting and receiving coils are axially aligned. Clearly, an angular or a lateral mis-alignment can drastically modify the mutual inductance (see Fig. 1(b)). In this case, it is not simple to evaluate M [10]. The same kind of consideration can be done about self-inductances L_t and L_r. In practice, coils may have a variety of geometric forms and characteristics imposed by design constraints. Apart from simple geometric forms (e.g. circular), it becomes complicated to provide analytic inductance expressions, which generally are approximated by simple models [6].

Path loss models comparison

In order to illustrate the differences addressed above, we provide path loss variations with distance, frequency, coil radius and the number of turns for the previously discussed models in addition to the “Modified-model” (eq (18)). The objective here is not to test a specific configuration but to check the validity of the different models and compare and verify their path losses in the same configuration.

Figure 3 gives the variations of path loss with distance at 13.56 MHz, in models 1, 2 and 3, and in our modified model. Model-1 gives the highest path loss while Model-3 gives the lowest one. The difference between the models in dB is significant since the approximations and the inductance expressions are quite different. Model-2 and the Modified-model are very close, except for small distances. For the set of parameters we used, Models 1, 2 and 3 show negative path loss values which are a consequence of the assumption in eq (12). Figure 4 shows a set of similar performances, but for a higher number of turns, in order to confirm the previous observations. We also notice that Model-1 and Model-3 largely overestimate the path loss while Model-2 fails to cover this set of parameters.

Figures 5 and 6 show the path loss as a function of frequency at distances 0.01 and 0.1 m, respectively. We observe that for all models, the path loss decreases with frequency. Model-3 always overestimates the path loss while Models 1 and 2 fail to cover this set of parameters and show negative path loss values. Only the Modified-model presents a quasi-constant path loss as a function of the frequency and under load matching condition.

In Figure 7 we can see that the path loss decreases with receiving coil radius while the differences between the models are significantly large. Figures 8 and 9 give path loss variations as a function of the number of turns in the transmitting coil for two different values of transmitting coil radius. We note that according to Model-3, the path loss increases with the number of turns of the transmitting coil contrarily to the other models. For a different transmitting coil radius (Figure 9) the same models-1 and Model-2 give negative path loss values while the modified-Model gives more accurate path loss values.

Similar observations can be made concerning the variations in path loss with receiving coil radius and number of turns (figures 7 to 9). We note that according to Model-3, the path loss increases with the number of turns in the transmitter or the receiver. In figure 10 we observe the same behaviour as Model-2 in the variation of the path loss as a function of the number of turns in the receiving coil.

According to these results, only the Modified-Model is able to give valid results for all configurations. This is more critical when other coil geometry and positionning are used.

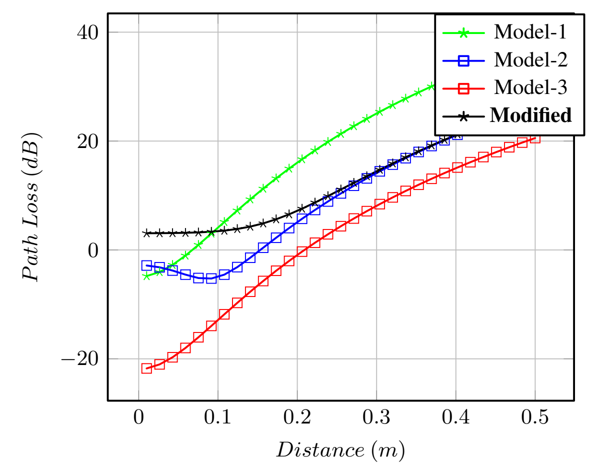

Fig. 3. Path Loss with distance for different models at 13.56 MHz, $a_t = 0.1$, $a_r = 0.1$, $N_t = 1$, $N_r = 1$

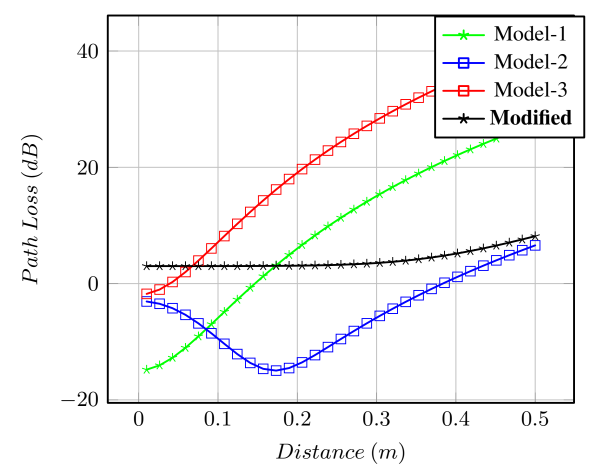

Fig. 4. Path Loss with distance for different models at 13.56 MHz, $a_t = 0.1$, $a_r = 0.1$, $N_t = 10$, $N_r = 10$

The variations of the path loss directly impact the performance of the system. Our model reflects the behaviour in a more realistic situation. This model will be used to establish

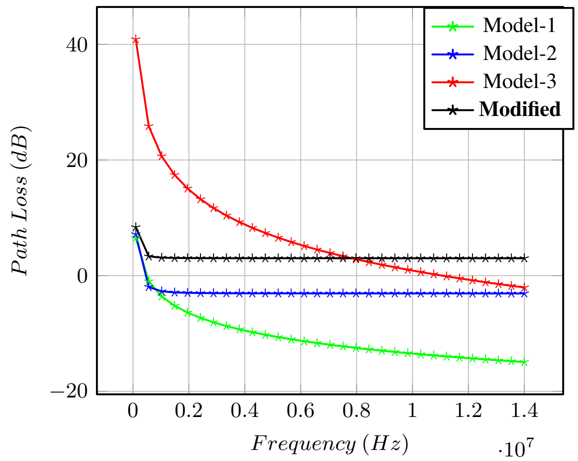

Fig. 5. Path Loss for different models with frequency from 0.1 to 15 MHz at a distance of 0.01 m, $a_t = 0.1$, $a_r = 0.1$, $N_t = 10$, $N_r = 10$

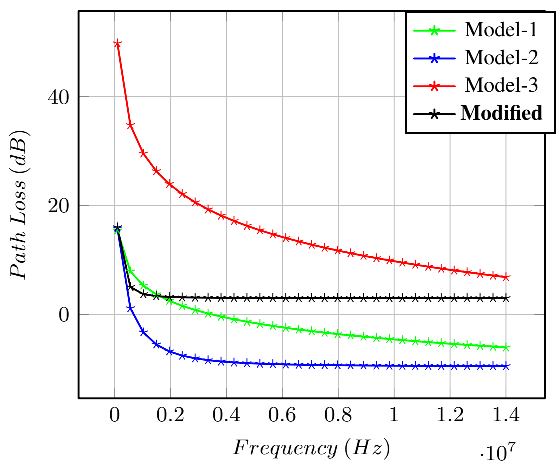

Fig. 6. Path Loss for different models with frequency from 0.1 to 15 MHz at a distance of 0.1 m, $a_t = 0.1$, $a_r = 0.1$, $N_t = 10$, $N_r = 10$

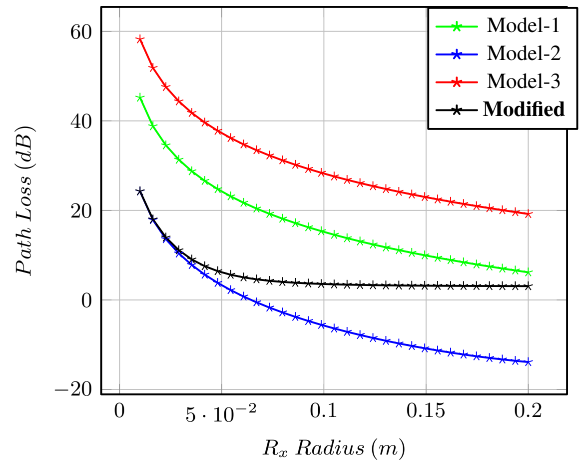

Fig. 7. Path Loss for different models with receiving coil radius a_r between 0.01 and 0.2 (m) at 13.56 MHz and a distance of 0.1 m, $a_t = 0.1$, $a_r = 0.1$, $N_t = 10$, $N_r = 10$

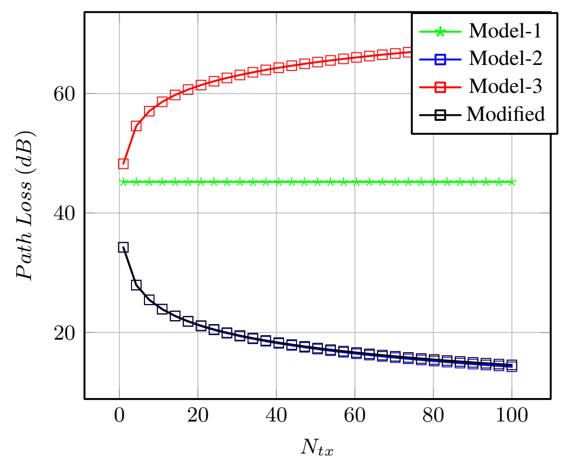

Fig. 8. Path Loss for different models with the number of turns in Rx coil between 1 and 100 turns at 13.56 MHz and a distance of 0.1 m, $a_t = 0.01$, $a_r = 0.01$, $N_r = 10$

the performance of an ASK binary transmission system in reference [6], where we assume a simple path loss model for the additive white gaussian noise channel.

Since distance is the major limiting factor of MI communications, one way to increase system coverage is to use relays which consist on a series of coils retransmitting the signal, sometimes also called 'waveguides'. Relay networks may be a very interesting solution for system coverage extension in environments where access is not possible or very costly, such as underwater or soil [5]. In this case, the global power ratio is the product of the power ratios for each couple of interacting coils. Consequently, the use of accurate path loss expression becomes more crucial. In reference [6], we investigate the performance of our accurate model for the relayed system.

IV. Conclusion

In this work, we have considered path loss models for MI communications. The behaviour of the EM wave in the near field cannot be modelled in a simple form. The vast majority of the models used to estimate the performance relies on some approximations of the magnetic coupling. The simplicity of the models not necessarily reflects the physics of the propagation in the near field, leading to inaccurate results. According to these results, only our Modified-model is able to give valid results for all configurations.

Appendix A
Path loss calculation

From equation (9), we can calculate the transmitted power as:

$$P_t(d) = Re(V_1 I_1^*) = Re(Z_{11} - \frac{Z_{12}^2}{Z_L + Z_{22}})|I_1|^2.$$

Also, from equation (10), we can calculate the received power as:

$$P_r = Re(Z_L)|I_2|^2 = Re(Z_L)\frac{|Z_{12}|^2}{|Z_L + Z_{22}|^2}|I_1|^2.$$

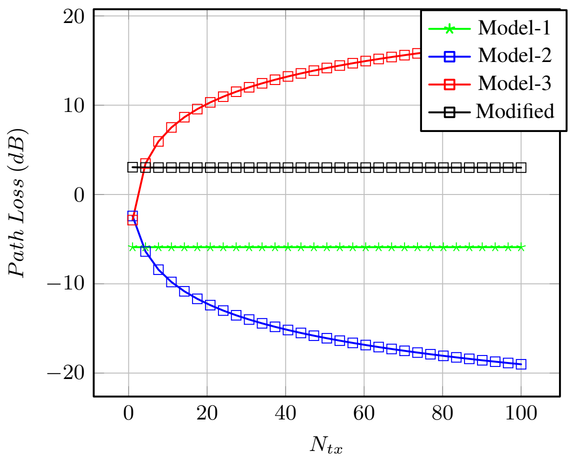

Fig. 9. Path Loss for different models with the number of turns in Rx coil between 1 and 100 turns at 13.56 MHz and a distance of 0.1 m, $a_t = 0.1$, $a_r = 0.1$, $N_r = 10$

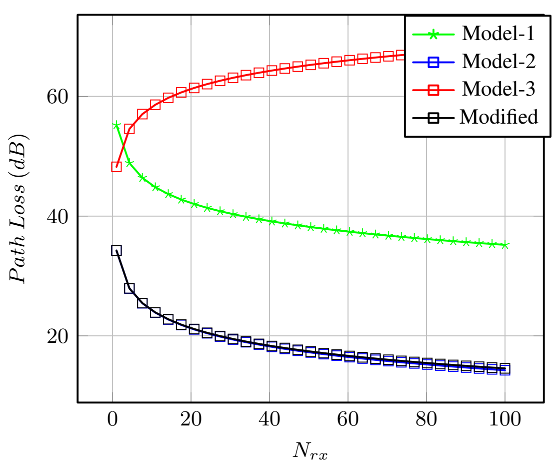

Fig. 10. Path Loss with the number of turns in the Rx coil for different models

Following these expressions, we derive the path loss:

$$
\begin{aligned}
PL &= \frac{P_r}{P_{t(d)}} \\
&= Re(Z_L)\frac{|Z_{12}|^2}{|Z_L + Z_{22}|^2}\frac{1}{Re(Z_{11} - \frac{Z_{12}^2}{Z_L + Z_{22}})}.
\end{aligned}
$$

Using definitions (11):

$$
\begin{aligned}
&Re(Z_{11} - \frac{Z_{12}^2}{Z_L + Z_{22}}) = \\
&\quad = Re(R_t + j\omega L_t - \frac{(j\omega M)^2}{R_L + jX_L + Rr + j\omega L_r}) = \\
&\quad = Re(R_t + j\omega L_t + \frac{\omega^2 M^2}{(R_L + Rr) + j(X_L + \omega L_r)}) =
\end{aligned}
$$

$$
\begin{aligned}
= Re(R_t + &\frac{\omega^2 M^2 (R_L + R_r)}{(R_L + R_r)^2 + (X_L + \omega L_r)^2} \\
&+ j(\omega L_t - \frac{\omega^2 M^2 (X_L + \omega L_r)}{(R_L + R_r)^2 + (X_L + \omega L_r)^2})) =
\end{aligned}
$$

$$
= R_t + \frac{\omega^2 M^2 (R_L + R_r)}{(R_L + R_r)^2 + (X_L + \omega L_r)^2}.
$$

$$
|Z_{12}|^2 = \omega^2 M^2,
$$

$$
|Z_L + Z_{22}|^2 = (R_L + R_r)^2 + (X_l + \omega L_r)^2.
$$

Using these expressions we obtain:

$$
PL = \frac{R_L \omega^2 M^2}{\begin{array}{r} R_t(R_L + R_r)^2 + R_t(X_L + \omega L_r)^2 \\ + \omega^2 M^2 (R_L + R_r) \end{array}}.
$$

REFERENCES

[1] "The internet of things," MIT Technology Review, July/August 2014.
[2] "Clrc663, mfrc631, mfrc 630, slrc610 low power card detection," NXP Application Note AN11145, May 2015.
[3] S. Mikki and Y. Antar, "A theory of antenna electromagnetic near field–part 1," *IEEE Trans. Antennas Propag.*, vol. 59, no. 12, pp. 4691–4705, Dec 2011.
[4] J. Sojdehei, P. Wrathall, and D. Dinn, "Magneto-inductive (mi) communications," in *OCEANS, 2001. MTS/IEEE Conference and Exhibition*, vol. 1, 2001, pp. 513–519 vol.1.
[5] B. Gulbahar and O. Akan, "A communication theoretical modeling and analysis of underwater magneto-inductive wireless channels," *Wireless Communications, IEEE Transactions on*, vol. 11, no. 9, pp. 3326–3334, September 2012.
[6] A. Charaf and G. R. Guisantes, "Near field channel models derived from electromagnetics," to be published.
[7] Z. Sun and I. Akyildiz, "Underground wireless communication using magnetic induction," in *Communications, 2009. ICC '09. IEEE International Conference on*, June 2009, pp. 1–5.
[8] M. Domingo, "Magnetic induction for underwater wireless communication networks," *IEEE Trans. Antennas Propag.*, vol. 60, no. 6, pp. 2929–2939, June 2012.
[9] J. Agbinya and M. Masihpour, "Magnetic induction channel models and link budgets: A comparison between two agbinya-masihpour models," in *Communications and Electronics (ICCE), 2010 Third International Conference on*, Aug 2010, pp. 400–405.
[10] S. Babic, F. Sirois, and C. Akyel, "Validity check of mutual inductance formulas for circular filaments with lateral and angular misalignments," *Progress In Electromagnetics Research*, vol. 8, pp. 15–26, 2009.